Phys Chem Minerals (2012) 39:169–176
DOI 10.1007/s00269-011-0472-x

ORIGINAL PAPER

Structure of magnetite (Fe_3O_4) above the Curie temperature: a cation ordering study

Davide Levy · Roberto Giustetto · Andreas Hoser

Received: 6 June 2011 / Accepted: 28 November 2011 / Published online: 10 December 2011

Abstract A pristine magnetite (Fe_3O_4) specimen was studied by means of Neutron Powder Diffraction in the 273–1,073 K temperature range, in order to characterize its structural and magnetic behavior at high temperatures. An accurate analysis of the collected data allowed the understanding of the behavior of the main structural and magnetic features of magnetite as a function of temperature. The magnetic moments of both tetrahedral and octahedral sites were extracted by means of magnetic diffraction up to the Curie temperature (between 773 and 873 K). A change in the thermal expansion coefficient around the Curie temperature together with an increase in the oxygen coordinate value above 700 K can be observed, both features being the result of a change in the thermal expansion of the tetrahedral site. This anomaly is not related to the magnetic transition but can be explained with an intervened cation reordering, as magnetite gradually transforms from a disordered configuration into a partially ordered one. Based on a simple model which takes into account the cation-oxygen bond length, the degree of order as a function of temperature and consequently the enthalpy and entropy of the reordering process were determined. The refined values are $\Delta H^0 = -23.2(1.7)$ kJ mol^{-1} and $\Delta S^0 = -16(2)$ J K^{-1} mol^{-1}. These results are in perfect agreement with values reported in literature (Mack et al. in Solid State Ion 135(1–4):625–630, 2000; Wu and Mason in J Am Ceramic Soc 64(9):520–522, 1981).

D. Levy (✉) · R. Giustetto
Dipartimento di Scienze Mineralogiche e Petrologiche, Università degli Studi di Torino, Via Valperga Caluso 35, 10125 Turin, Italy
e-mail: davide.levy@unito.it

A. Hoser
Helmholtz Zentrum Berlin, BENSC, 14109 Berlin, Germany

Keywords Magnetite · Neutron powder diffraction · Cation partitioning · Magnetic order

Introduction

Magnetite is the first magnetic material known since the ancient times. Its structure, formally $Fe^{II}Fe^{III}_2O_4$, is spinel-like (Fleet 1981, 1986) and is derived from an oxygen cubic close packing with cations in the interstitial tetrahedral and octahedral sites. This kind of structure, ideally cubic, is typical of many AB_2O_4 compounds, where A is usually a bivalent cation and B a trivalent one. Two limit-configurations are possible: in the so called normal structure, the A and B cations fill the tetrahedral and octahedral sites, respectively, whereas in the 'inverse' one, the tetrahedral sites are filled by half B cations while the residual half of B and all A cations disorderly fill the octahedral sites. The study of cation partitioning in spinels is widely used in geology to understand the genesis of these phases in natural rocks, but it is also useful in the study of their physical properties in materials science. Magnetite is a typical inverse spinel (Verwey and Haayman 1941) in which Fe(II) and Fe(III) are disordered in the octahedral sites, while the tetrahedrons are fully occupied by Fe(III) cation. From the point of view of the magnetic properties, magnetite has a Verwey ordering at low temperature ($T_v = 118$ K) (Verwey and Haayman 1941) and it is ferrimagnetic up to the Curie temperature, at about 856 K (Néel 1948); above such values, it becomes paramagnetic (Shull et al. 1951). The ferrimagnetism is due to an antiferromagnetism coupling of Fe(III) in tetrahedral and octahedral sites. Recently, magnetite has become an important technological material as a nanomagnetic

component (Poddar et al. 2002). A peculiar behavior shown by magnetite was discovered by Rozenberg et al. (2007) at high pressure, who found that above 20 GPa an enlargement of the tetrahedral site became highlighted. This occurrence was possibly referred to a structural transition of this phase from *inverse* to *direct* spinel. As a matter of fact, the Fe^{2+}–O bond length is bigger than the Fe^{3+}–O bond length in tetrahedral sites: 2.03 and 1.89 Å, respectively (Shannon 1976).

An in-depth study of the structure of magnetite at high temperature is limited by the strong Fe(II) predisposition to be oxidized when heated above 373 K, even in the presence of very small oxygen quantities (personal observation). Despite this difficulty, some studies concerning the high-temperature structural behavior of magnetite were reported. A cation distribution study on magnetite at high temperature was performed using thermopower measurements (Wu and Mason 1981), revealing that a partial ordering of the spinel structure starts at 858 K, and proceeds until the melting temperature is reached (1,773 K). The maximum percentage of direct spinel structure detected at the highest temperature was 35%. The same results were achieved by using Mössbauer spectroscopy (Wissmann et al. 1998). A structural work on magnetite at high temperature was also made by using a X-ray single crystal (Okudera et al. 1996), showing no significant structural changes in magnetite below the Curie temperature. Unfortunately, no data have been reported for higher temperatures. Another structural work at high temperature (Mazzocchi and Parente 1998), performed by using neutron multiple diffraction data on a single crystal, gave a description of the magnetite structure at 976 K but included no discussion on a possible cation partitioning. In a previous work (Levy et al. 2004), it was stated that the thermal expansion coefficient shows a change at the Curie temperature in a slightly oxidizing environment (an effect usually referred to as the 'loss of the magnetostriction'), whereas the same coefficient evidences no variation in a reducing atmosphere. The aim of this work is to describe the effect of the Curie magnetic transition on the structure of magnetite and to study and explain the variation in the thermal expansion coefficient at high temperature from a structural point of view.

Experimental

Sample

This study was performed on a natural magnetite sample collected in the Brosso mining area in Ivrea, Italy. The specimen was purified from the rock matrix by means of magnetic separation. SEM–EDS chemical analyses, performed using a Cambridge Stereoscan 360 SEM equipped with Oxford INCA Energy 200 microanalysis and Pentafet EDS detector, showed this magnetite sample to be almost completely pure with a maximum of 3% Mg atoms per formula unit. X-ray powder diffraction (XRPD) analysis performed with a PANanalytical X'Pert diffractometer showed that all diffraction peaks were related to the magnetite, and no further impurities were detected. The calculated cell edge [$a = 8.3957(5)$ Å] is consistent with the values reported in literature (Fleet 1981, 1986).

Neutron powder diffraction data collection and analysis

The sample was studied by means of neutron powder diffraction (NPD) at high temperature. Diffraction data were collected at the Helmholtz-Zentrum, Berlin (HZB, Germany) with BER-II neutron source by means of an angle dispersion diffraction experiment on the E2 diffractometer.

The powder, contained in a quartz tube sample holder, was heated in situ by means of a furnace in high vacuum starting at room temperature (298 K) and progressively increasing by 100 K steps (except the first one, equal to 75 K) until $T = 1{,}073$ K was reached. The data collection time for each temperature step was 4 h.

As expected, in the collected neutron diffraction patterns, some selected peaks show a systematic intensity decrease with temperature rise (as shown in Fig. 1), namely (111) ($d_{111} = 4.84$ Å), (222) ($d_{222} = 2.42$ Å), (331) ($d_{331} = 1.93$ Å) and (531) ($d_{531} = 1.42$ Å). The intensity of such reflections is strongly dependent from temperature, as below the Curie temperature these peaks are clearly visible whereas above they possess very small

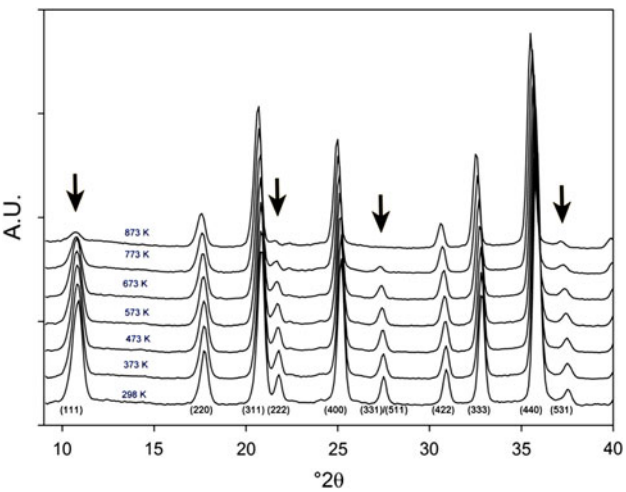

Fig. 1 Neutron powder diffractogram of the S2 sample collected at BER-II neutron source, E2 diffractometer, from 298 to 873 K. *Arrows* indicate the diffraction peaks, which contribute the higher magnetic diffraction

or no intensity, acting therefore as good markers for the magnetic–paramagnetic transition. At all studied temperatures, however, all detectable diffraction peaks can undoubtedly be indexed by using the magnetite cubic cell. The magnetic structure of magnetite corresponds therefore to the cubic one, typical of the atomic structure.

NPD data were refined using GSAS/EXPGUI (Larson and Von Dreele 2004; Toby 2001) software. To refine the atomic structure of magnetite, consistently with literature data (Fleet 1986), the space group $Fd\bar{3}m$ was used and the cation positions fixed at (1/2, 1/2, 1/2) and (1/8, 1/8, 1/8) for the octahedral and tetrahedral sites, respectively. Starting fractional coordinates for the oxygen atom were set at (0.255, 0.255, 0.255).

In order to describe the intensity of the magnetic diffraction peaks, a magnetic phase was added to the model for further refinement with the Rietveld method. As no in-depth description was found for such a phase, a cubic model was used with the same cell edge of the atomic phase. In order to describe in a simple way this magnetic structure, a F-1 symmetry was chosen: the octahedral cations were positioned at (1/2, 1/2, 1/2), (1/2, 3/4, 3/4), (3/4, 1/2, 3/4) and (3/4, 3/4, 1/2) and the tetrahedral ones in the same position of the atomic phase. A unitary magnetic vector was defined for each atom along the (111) direction; the magnetic vector for the octahedral site proved to be anti-parallel with respect to the tetrahedral one, as shown in Fig. 2.

The peak profiles were modeled using a pseudo-Voigt function, varying the three terms Caglioti formula of the profile curve Gaussian part and the Lx and Ly parameters of the Lorentzian part. Asymmetry and shift parameters were also refined. A shifted Chebyshev function with 20 terms was used to interpolate the background. The two-theta offset was refined only for the room temperature diffractogram, and the obtained value used also for the other diffraction patterns.

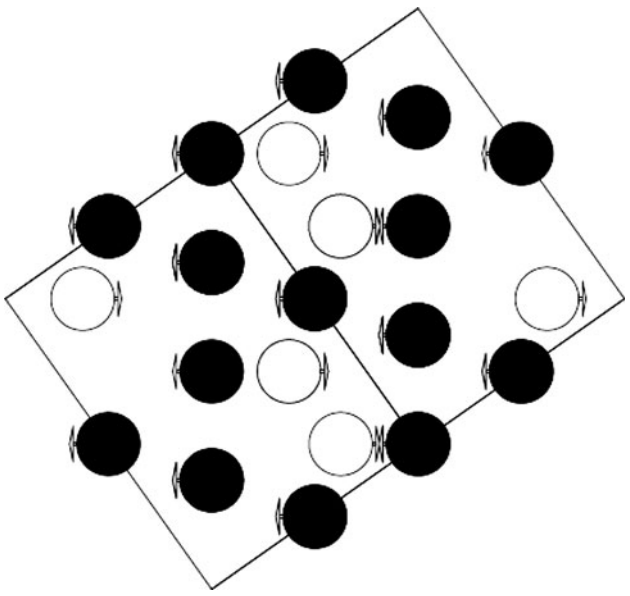

Fig. 2 Magnetic structure of magnetite along the (011) plane. *Black* and *white circles* represent Fe in the octahedral and tetrahedral sites, respectively

In the structure of magnetite, the only refinable atomic parameter is the unique fractional coordinate of the oxygen atom. In addition, other refined parameters are the isotropic displacements of both the oxygen and iron atoms and, in certain cases, the site occupancy of iron (in order to check the possible oxidation of the phase, as discussed below).

As reported by Wright et al. (2001), neutron powder data for a cubic phase are insensitive to the moment directions as only their relative intensity affects the magnetic diffraction intensities. For such a reason, the magnetic moment components were constrained to be anti-parallel in the tetrahedral and octahedral sites and they were allowed only to vary the magnitude. Above 773 K, the peaks related to the magnetic structure disappear from the diffraction patterns; the related magnetic moments could therefore be refined no further. Such a step is reputed to indicate the crossing of the Curie temperature.

Refined structural data are reported in Table 1. It is evident that the refined parameters at room temperature are not congruent with those found at higher temperatures or with the reference diffractogram collected at room temperature by means of conventional XRPD. The main discrepancies can be summarized as follows: (1) the cell edge determined by NPD is 8.3925(5) Å versus 8.3957(5) Å by XRPD and 8.3998(5) Å by NPD at 373 K; (2) the magnetization moment at room temperature for the tetrahedral site is not consistent with the values found at higher temperatures; (3) the refined values of the oxygen atom fractional coordinates at room temperature are higher than those refined in the temperature range 373–673 K. By taking into account these problems, it would seem that the room temperature neutron diffractogram may be affected by a small mismatch between low- and high-angle peak positions, probably due to a not perfect positioning of the sample before the vacuum reached the maximum. Such a mismatch is not possible to correct it by adopting the usual correction variables (zero shift and profile shift). This complication does not appear in the higher temperature diffractograms. In order to determine the correct value for these parameters at room temperature, the cell edge resulting from XRPD was taken into account while the tetrahedral magnetic moment and the oxygen position were extrapolated by taking into consideration the trend of the related curves at higher temperatures.

Table 1 Refined structural features of magnetite, from left to right: temperature of data collection, R error indexes on the whole profile and on F^2 of Bragg peaks, fractional coordinate of oxygen atom in the position (x, x, x), thermal parameters for Oxygen (O), Fe in octahedral site (M) and in tetrahedral site (T), cell edge a, x component of the magnetic vector M for the octahedral site (M) and tetrahedral site (T), magnitudes of magnetization for the two sites

T (K)	Rwp %	R (F2) %	x (O)	$U_{iso} \times 100$ (Å^2) (O)	$U_{iso} \times 100$ (Å^2) (M)	$U_{iso} \times 100$ (Å^2) (T)	a (Å)	M_x (μB) (M)	M_x (μB) (T)	M_{oct} (μB)	M_{tet} (μB)
298	5.51	3.09	0.2564(2)	0.0075(6)	0.0164(9)	0.0105(7)	8.3925(5)	2.16(6)	−2.40(8)	3.75(6)	4.17(8)
373	4.79	2.51	0.2558(2)	0.0100(7)	0.0130(9)	0.0107(7)	8.3998(5)	2.11(5)	−2.59(7)	3.66(5)	4.49(7)
473	4.57	2.36	0.2559(2)	0.0115(7)	0.0145(9)	0.0121(7)	8.4082(5)	1.99(5)	−2.50(7)	3.44(5)	4.32(7)
573	4.31	2.58	0.2559(2)	0.0133(7)	0.0162(9)	0.0134(7)	8.4190(4)	1.81(5)	−2.35(7)	3.12(5)	4.07(7)
673	4.21	2.60	0.2559(2)	0.0154(7)	0.0175(9)	0.0149(7)	8.4324(5)	1.53(6)	−2.12(8)	2.66(6)	3.67(8)
773	3.99	2.64	0.2563(2)	0.0177(8)	0.0202(9)	0.0169(7)	8.4499(5)	0.93(8)	−1.5(1)	1.62(8)	2.7(1)
873	4.07	2.28	0.2567(2)	0.0194(8)	0.0221(9)	0.0191(7)	8.4689(5)	–	–		
973	3.89	2.19	0.2567(2)	0.0215(8)	0.0233(9)	0.0213(8)	8.4814(5)	–	–		
1,073	3.78	2.41	0.2571(2)	0.0233(8)	0.026(1)	0.0228(8)	8.4937(5)	–	–		

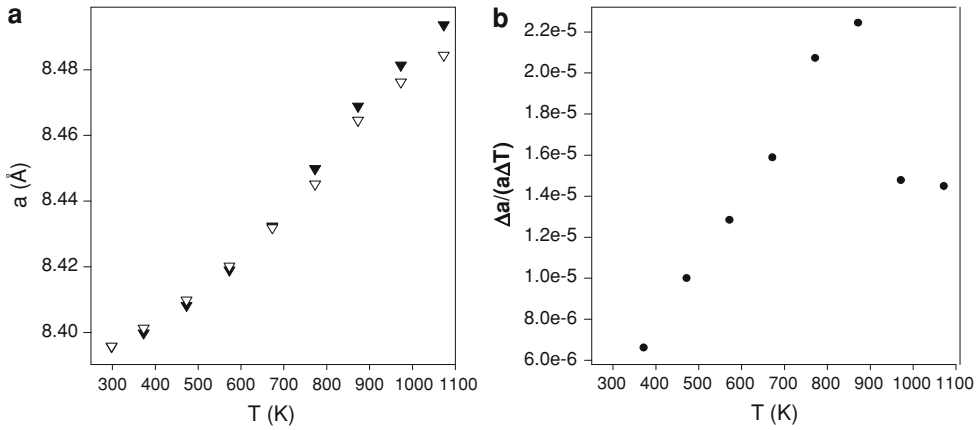

Fig. 3 In **a** the cell edge of magnetite is plotted versus temperature; *black triangles* are referred to data in this work, *white triangles* to data collected by means of X-ray powder diffraction (Levy et al. 2004). In **b** the thermal expansion coefficient, calculated by the formula $\alpha_{T_n} = \frac{(a_{T_n} - a_{T_{n-1}})}{a_{T_n}(T_n - T_{n-1})}$ as described in the text, is plotted at different temperatures. It has to be highlighted that both in **a** and in the thermal expansion calculation, the room temperature cell obtained by XRPD was used, due to the refinement problems affecting the RT data set

Results and discussion

Thermal expansion

The thermal expansion of the studied magnetite sample cell edge is reported in Fig. 3a, together with the cell edge thermal expansion of a different specimen previously collected by means of X-ray powder diffraction (Levy et al. 2004) under similar experimental conditions. Differences between these two curves are mainly due to different degrees of oxidation, as the sample collected with X-ray powder diffraction is reported to be slightly oxidized at the end of thermal cycle.

The thermal expansion of any material is thermodynamically defined by the following differential equation: $\alpha = \frac{\delta X}{X(\delta T)}$, where X is the expanding parameter (volume or cell edge) and T the temperature. Due to the fact that from an experimental point of view the adopted temperature intervals have finite differences, the thermal expansion coefficient for magnetite was calculated for the different temperature steps using the following formula:

$$\alpha_{T_n} = \frac{(a_{T_n} - a_{T_{n-1}})}{a_{T_n}(T_n - T_{n-1})},$$

where a_{T_n} is the cell edge at the nth temperature value (T_n) and $a_{T_{n-1}}$ the cell edge at the previous temperature value. The corresponding plot is reported in Fig. 3b.

It has to be pointed out that both in Fig. 3a and in the thermal expansion calculation, the value of the cell obtained by XRPD at room temperature was used, for the reason given above. The thermal expansion linearly increases with temperature up to 673 K. Above such a

value, a more drastic growth can be observed until a maximum is reached at 873 K, at which point the magnetic peaks in the diffractogram disappear. Such a discontinuity is symptomatic of a phase transition and is often referred to the 'loss of magnetostriction'. As exhaustively discussed below, however, such a change cannot be related to the magnetic transition but rather to an intervened cation partitioning.

Magnetic refinement

The refinement of the iron atoms magnetic moments was calculated by adopting the module of the three components of the magnetic vector (as described above). The total magnetization was obtained as the difference between the double of the octahedral magnetization and the tetrahedral one; the latter condition is dictated by the fact that the cations in octahedrons are twice as much those in tetrahedrons. The resulting values are reported in Table 1 and plotted in Fig. 4. The room temperature magnetic moments in the octahedral and tetrahedral sites are 3.75(6) μB (refined experimental value) and 4.56 μB (extrapolated value), respectively. These results can be compared with those determined by Klotz et al. (2008) on a synthetic sample studied from room to high pressure, whose values were slightly lower at room pressure [3.60(6) and 4.05(4) μB for the octahedral and tetrahedral sites, respectively]. This divergence could be explained by both the different origin of the specimens (the sample analyzed in the current study being natural whereas a synthetic one was used by Klotz et al. 2008) and the experienced difficulties in sharply refining such parameters due to their high sensibility to small structural variations.

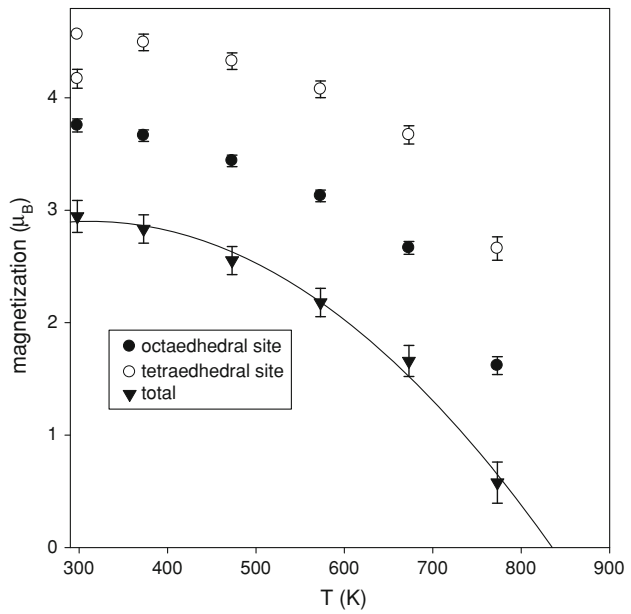

Fig. 4 Magnetization of Fe in the two crystallographic sites versus temperature. The *black* and *white circles* represent the magnetization of the octahedral and tetrahedral sites, respectively, the *black triangles* the total magnetization. Note that the room temperature value of the tetrahedral magnetization was extrapolated by the higher temperature data, because the former are not coherent with high-temperature behavior. Experimental data symbols are shown with *error bar*; extrapolated data bring none

The thermal evolution of the magnetic moments shows a significant decrease with temperature rise, in agreement with the previously mentioned intensity fall of the magnetic peaks. Using a quadratic polynomial function, it is possible to fit the total magnetization, thus extrapolating a feasible value for the Curie temperature. By using this procedure, the Curie temperature proved to be 838 K, in good agreement with the literature value (Néel 1948). Such a threshold indicates that the magnetite structure, as expected, shows no magnetic order above the Curie temperature.

Structure refinement

As previously explained, the spinel structure has only one degree of freedom: the position of the oxygen atom, for which all three fractional coordinates are equal (x, x, x). The other refined parameters are the isotropic thermal parameters of oxygen and iron ions in the related structural sites. As expected, the values of the thermal parameters increase proportionally with temperature rise due to an increase in the thermal motion. The occupancies of iron atoms were refined in a preliminary stage to check any possible compositional variation during heating, but in the end they were fixed to their ideal values as no significant variation was found at high temperature. Due to the high sensibility of neutron diffraction for the atom occupancy values, it is reliable to assess that throughout the adopted temperature ramp (from room temperature to the highest measured value), the studied specimen has maintained its original ideal formula and no oxidation has occurred. Unfortunately, no measurement could be performed on the cooled sample after the heating treatment was over, as the furnace was inadvertently opened before room temperature was reached, thus causing an undesirable specimen oxidation. The values of the refined structural parameters are reported in Table 1, together with the related standard deviations and refinement error indexes.

By carefully examining Fig. 5, it appears evident how the oxygen coordinate remains constant when temperature is below 700 K, whereas at higher temperatures this value increases. The described behaviors for both the oxygen coordinate and cell edge expansion can be explained by analyzing the dimensions of the tetrahedral and octahedral coordination polyhedrons. In Fig. 6, the cation-oxygen bond lengths are plotted for different temperatures in the

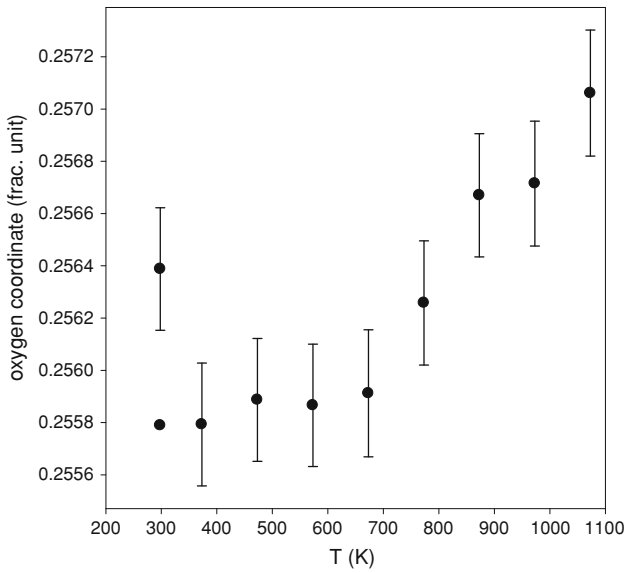

Fig. 5 Coordinate of the oxygen ion versus temperature. Note that the room temperature value of the oxygen coordinate was corrected by linear interpolation of the data between 373 and 673 K. Experimental data symbols are shown with *error bar*; extrapolated data bring none

Table 2 Calculated bond lengths of cation-oxygen bonds in octahedral (M–O) and tetrahedral (T–O) sites and Fe(II) in tetrahedral site

Temperature (K)	M–O (Å)	T–O (Å)	Fe(II) in tetrahedron
298 (calculated)	2.0459(1)	1.90992(8)	
298 (extrapolated)	2.0514(1)	1.90214(8)	0.08
373	2.0525(1)	1.90291(8)	0.07
473	2.0538(1)	1.90627(8)	0.08
573	2.0566(1)	1.90833(8)	0.07
673	2.0595(1)	1.91205(8)	0.08
773	2.0610(1)	1.92118(8)	0.13
873	2.0623(1)	1.93142(8)	0.18
973	2.0650(1)	1.93494(8)	0.19
1,073	2.0652(1)	1.94282(8)	0.22

The last values are obtained by comparing the Fe–O bond lengths and the observed tetrahedral thermal expansion with the tabulated value of Fe(II) and Fe(III) cation radii, as reported in the text

octahedral and tetrahedral sites (panel A and B, respectively; notice that the scale of bond lengths on the *Y* axes is the same for both graphs in order to highlight the different behaviors). It can be noted that below 673 K, the thermal expansion of the two coordination polyhedrons is quite similar, while above this temperature, the tetrahedron expansion is definitely higher than that of octahedron. Above 673 K, the octahedron dimensions increase quite monotonically, whereas the tetrahedral site shows a significant change in the thermal expansion. This behavior indicates that a temperature-dependent cation reordering might occur. As already shown by Rozenberg et al. (2007), in tetrahedral coordination, Fe(II) has a bigger cation radius with respect to Fe(III) (0.63 Å vs. 0.49 Å) (Shannon 1976), while in the octahedral coordination, the radii of the two cations are similar (0.61 Å and 0.645 Å for Fe(II) and Fe(III), respectively). Considering that the oxygen ionic radius is 1.38 Å and that, at room temperature, equal quantities of Fe(II) and Fe(III) occupy the octahedral site, the Fe(III)-O bond length in tetrahedron should be 1.87 Å and [Fe(II),Fe(III)]–O in octahedron vary between 1.99 and 2.025 Å. These theoretical values are not very different from those experimentally determined at room temperature (see Table 2).

Neutron diffraction cannot directly discriminate the Fe(II)/Fe(III) partitioning, the two cations having the same neutron cross section. An indirect method has therefore to be used in order to evaluate how cation partitioning behaves in magnetite by means of neutron diffraction data; in this work, the variation in the bond lengths was analyzed. At high temperature, the bond length variation in spinel is due to two main causes: thermal expansion and cation partitioning. As the tetrahedral site appears to be more sensitive to Fe(II)/Fe(III) exchange (see the above-mentioned considerations on cation dimensions), the

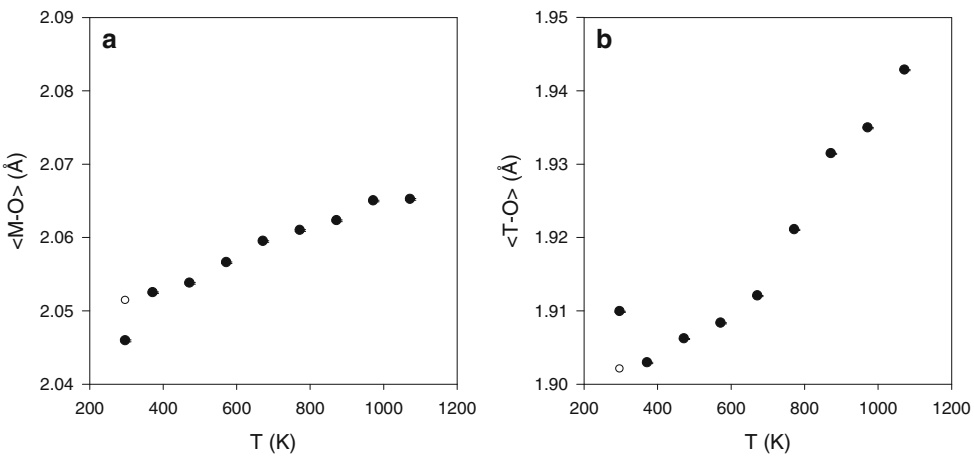

Fig. 6 Oxygen coordinate versus temperature. In **a**, the octahedral cation-oxygen bond length is plotted versus temperature; in **b**, the tetrahedral one is reported. Note that the room temperature value of the oxygen coordinate was also calculated using the corrected cell edge and oxygen coordinate value (*white circle*)

following methodology was used to determine the cation partition of iron:

1. The thermal expansion of the tetrahedron is hypothesized to be linear and determined on the basis of the bond length values in the 298 and 673 K temperature range, in which the expansion is linear. A plausible hypothesis is that such expansion does not change during the cation reordering; such an assumption can be considered sufficiently valid due to the scarce presence of the Fe(II) cation in the tetrahedral site.
2. The differences between the experimental and calculated bond lengths are determined using the thermal expansion values according to the procedure described in previous point 1.
3. The values found at point 2 were summed to the experimental bond lengths measured at room temperature, in order to possibly determine the bond lengths values at different temperatures without the thermal expansion contribution.
4. A linear correlation between the tetrahedral bond length and Fe(II) occupancy was hypothesized, using the following formula:

   $$\mathrm{TBL} = x\mathrm{F2BL} + (1-x)\mathrm{F3BL},$$

   where x is the site occupancy for Fe(II), TBL is the tetrahedral bond length determined as previously reported, F2BL and F3BL are the bond lengths for Fe(II)–O and Fe(III)–O as reported in literature for the tetrahedral coordination (Shannon 1976).
5. To obtain the Fe(II) occupancy, the above-mentioned equation is solved as a function of x: $x = \frac{(\mathrm{TBL}-\mathrm{F3BL})}{(\mathrm{F2BL}-\mathrm{F3BL})}$.

In this way, the Fe(II) occupancy in the tetrahedral site was determined for each experimental temperature stage; the obtained values are reported in Table 2 and plotted in Fig. 7. Despite the fact that this method has not been calibrated with other spinels, the result is similar to that found by thermopower and Mössbauer techniques (Wissmann et al. 1998; Wu and Mason 1981).

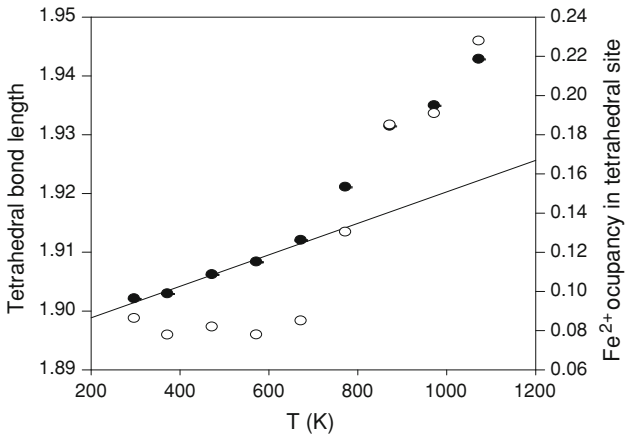

Fig. 7 *Black circles* are the tetrahedral bond length; the *continuous line* is the linear regression of the tetrahedral thermal expansion computed on the first five points; *white circles* are the quantity of Fe(II) in tetrahedral coordination polyhedron

From a thermodynamic point of view, the chemical formula describing the cation partitioning in magnetite can be expressed as:

$$\mathrm{Fe_T(II)} + \mathrm{Fe_O(III)} \Leftrightarrow \mathrm{Fe_O(II)} + \mathrm{Fe_T(III)}$$

where the indexes T and O are referred to the iron in the tetrahedral and octahedral sites, respectively. Using this formula, the equilibrium constant K_{CD} is defined after Mack et al. (2000) as:

$$K_{CD} = \frac{\lambda^2}{(1-\lambda)(2-\lambda)} = \exp\left(-\frac{\Delta G^0}{RT}\right) = \exp\left(\frac{\Delta S^0}{R}\right)\exp\left(-\frac{\Delta H^0}{RT}\right)$$

where λ is the quantity of Fe(III) in tetrahedral site, T the temperature in Kelvin, R the perfect gas constant and ΔG, ΔS and ΔH are the Gibbs energy, entropy and enthalpy, respectively. The refined values of entropy and enthalpy for temperatures between 673 and 1,073 K are $\Delta H^0 = -23.2(1.7)$ kJ mol^{-1} and $\Delta S^0 = -16(2)$ J K^{-1} mol^{-1}. This result falls perfectly in line with the values reported by Wu and Mason (1981) and Mack et al. (2000), thus confirming the reliability of the adopted method to evaluate the magnitude of the cation partition in magnetite by means of neutron powder diffraction.

Conclusions

The anti-ferrimagnetic ordering of magnetite was observed up to 773 K by neutron powder diffraction, confirming that the Curie transition is correlated to a loss of the magnetic ordering between 773 and 873 K. For the first time, the magnetization of octahedral and tetrahedral sites for magnetite was determined up to the Curie temperature by means of a refinement of the magnetic structure using the Rietveld method. By fitting the collected experimental data, the Curie temperature proved to be 838 K, with little variance with respect to the values reported in literature (856 K).

Above the Curie temperature, the expansion in the dimensions of the tetrahedral polyhedrons shows an anomaly that we assume to be due to the cation partitioning. The tetrahedral site has shown a more enhanced sensibility for such a parameter, due to the fact that the bigger Fe(II) cation enters the tetrahedron and the smaller Fe(III) moves to the octahedral site: the averaged difference in the Fe–O bond length calculated between the Fe(II) and Fe(III)

occupied tetrahedral sites is about 0.14 Å. By examining the expansion of this coordination site as a function of temperature and the theoretical and experimental cation-oxygen bond length, it was possible to determine the magnitude of the cation partitioning. Accordingly, the entropy and enthalpy values were also deduced. The obtained values for the thermodynamic parameters are in agreement with the reported entropy and enthalpy values, as determined by means of direct measurements of cation partition using Mossbauer spectroscopy (Mack et al. 2000).

The very large change in the tetrahedral site dimensions has proven to be the main cause in the variation in the thermal expansion parameter with temperature above the Curie transition. This shows that the variation in thermal expansion is not due to loss of magnetostriction, but instead to cation partitioning.

Acknowledgments The authors thank Dr. Pietro Vignola (IDPA-CNR, Milano Italy) for kindly providing the magnetite sample. This research project was supported by the European Commission under the 6th Framework Program through the Key Action: Strengthening the European Research Area, Research Infrastructures. Contract no.: RII3-CT-2003-505925 (NMI3). The authors are indebted to the reviewers for their suggestions that have really enhanced the original manuscript.

References

Fleet ME (1981) The structure of magnetite. Acta Crystallogr B37:917–920

Fleet ME (1986) The structure of magnetite: symmetry of cubic spinels. J Solid State Chem 62(1):75–82

Klotz S, Steinle-Neumann G, Strassle T, Philippe J, Hansen T, Wenzel MJ (2008) Magnetism and the Verwey transition in Fe3O4 under pressure. Phys Rev B 77(1):4. doi:10.1103/PhysRevB.77.012411

Larson AC, Von Dreele RB (2004) General structure analysis system (GSAS). Los Alamos National Laboratory Report, pp 86–748

Levy D, Artioli G, Dapiaggi M (2004) The effect of oxidation and reduction on thermal expansion of magnetite from 298 to 1173 K at different vacuum conditions. J Solid State Chem 177(4–5): 1713–1716

Mack DE, Wissmann S, Becker KD (2000) High-temperature Mössbauer spectroscopy of electronic disorder in complex oxides. Solid State Ion 135(1–4):625–630

Mazzocchi VL, Parente CBR (1998) Refinement of the ferri- and paramagnetic phases of magnetite from neutron multiple diffraction data. J Appl Crystallogr 31(5):718–725. doi:10.1107/S0021889898004324

Néel L (1948) Propriétés magnétiques des ferrites. Ferrimagnétisme et antiferromagnétisme. Anneles des Physique 3:137

Okudera H, Kihara K, Matsumoto T (1996) Temperature dependence of structure parameters in natural magnetite: single crystal X-ray studies from 126 to 773 K. Acta Crystallogr B 52:450–457

Poddar P, Fried T, Markovich G (2002) First-order metal-insulator transition and spin-polarized tunneling in Fe3O4 nanocrystals. Phys Rev B 65(17):172405

Rozenberg GK, Amiel Y, Xu WM, Pasternak MP, Jeanloz R, Hanfland M, Taylor RD (2007) Structural characterization of temperature- and pressure-induced inverse ↔ normal spinel transformation in magnetite. Phys Rev B 75(2). doi:10.1103/PhysRevB.75.020102

Shannon R (1976) Revised effective ionic radii and systematic studies of interatomic distances in halides and chalcogenides. Acta Crystallogr A 32(5):751–767. doi:10.1107/S0567739476001551

Shull CG, Wollan EO, Koehler WC (1951) Neutron scattering and polarization by ferromagnetic materials. Phys Rev 84(5):912–921

Toby BH (2001) EXPGUI, a graphical user interface for GSAS. J Appl Crystallogr 34:210–221

Verwey W, Haayman PW (1941) Electronic conductivity and transition point of magnetite. Physica 6(11):979–987

Wissmann S, Von Wurmb V, Litterst FJ, Dieckmann R, Becker KD (1998) The temperature-dependent cation distribution in magnetite. J Phys Chem Solids 59(3):321–330

Wright JP, Attfield JP, Radaelli PG (2001) Charge order structure of magnetite Fe3O4 below the Verwey transition. Phys Rev B 66(21):214422

Wu CC, Mason TO (1981) Thermopower measurement of cation distribution in magnetite. J Am Ceramic Soc 64(9):520–522